International Journal of Engineering in Computer Science

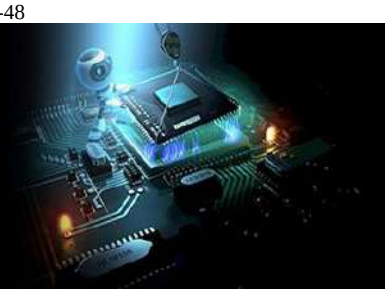

E-ISSN: 2663-3590
P-ISSN: 2663-3582
IJECS 2022; 4(2): 42-48
Received: 13-07-2022
Accepted: 26-08-2022

Obaje Samuel Enemakwu
Department of Computer Engineering, Federal Polytechnic, Offa, Nigeria

Correspondence Author;
Obaje Samuel Enemakwu
Department of Computer Engineering, Federal Polytechnic, Offa, Nigeria

Subjecting soleprint to fingerprint recognition algorithm treatment

Obaje Samuel Enemakwu

DOI: https://doi.org/10.33545/26633582.2022.v4.i2a.76

Abstract
This experiment was carried out to demonstrate that a Soleprint would easily substitute a fingerprint for identification and voting purposes for leprosy patients, injury victims, and natural causes who have no fingerprints. The fingerprint recognition algorithm was used throughout the experiment to conduct preprocessing stages such as segmentation, normalization, Gaussian blurring, noise reduction, Canny, Orientation, Binarization Thinning, Gabor Filtering, and Minutiae Extraction. These stages were performed on a Soleprint image and a Fingerprint image with the same properties of 8-bit grey-level, 600-dpi resolution, and scale 256 pixels, all in bitmap image compression format. Since the experiment was not designed to assess recognition algorithms, computation time was not considered. When the findings were compared, it was discovered that the algorithm has the same impact on both photos (Soleprint and Fingerprint, both whorl in class) and that the minutiae points are the basis for matching a fingerprint in today's trend, are also present on the Soleprint. A modern method of self-identity and voting for lepers and injury patients is now accessible.

Keywords: Leprosy, minutiae extraction, whorl, matching, soleprint, fingerprint

1. Introduction
Since a fingerprint is a pattern of ridges on the surface of a fingertip, a soleprint is a point on the sole adjacent to the big toe, at the flat space just behind the toes, that has features similar to a fingerprint and could be used for identification (Fig. 1). The soleprint impression could be achieved using standard inking techniques.
For quite some time, the fingerprint has become a significant source of authentication used in banks worldwide for cheque checking and voter registration. As common as these seem, cheque validation at banks or biometric identification systems assists in detecting irregularities that can occur at times and exercising our democratic right by voting at every stage. Unfortunately, certain individuals cannot use their fingerprints as a personal identity due to leprosy or an injury.

2. Proposed mode of identification
This experiment was needed because the Soleprint was found to have similar characteristics to the fingerprint, namely individuality to man. It, therefore, could be used to personally recognize a group of people who did not have fingerprints. Consequently, the soleprint was subjected to fingerprint recognition algorithm care (Fingerprint Picture Pre-processing and Minutiae Extraction) and compared to fingerprint images in the same class; the result supports the statement.

3. Methodology
For comparison purposes, the fingerprint recognition algorithm mentioned in (Jain *et al*., 2020; Chandan *et al*., 2020; Zhang, 2019; Hong, Wan, and Jain, 2021; Maltoni *et al*., 2018) [5, 2, 8, 3, 6] was used to evaluate both the Soleprint picture and a reference fingerprint image (the two images were of the same class, whorl).

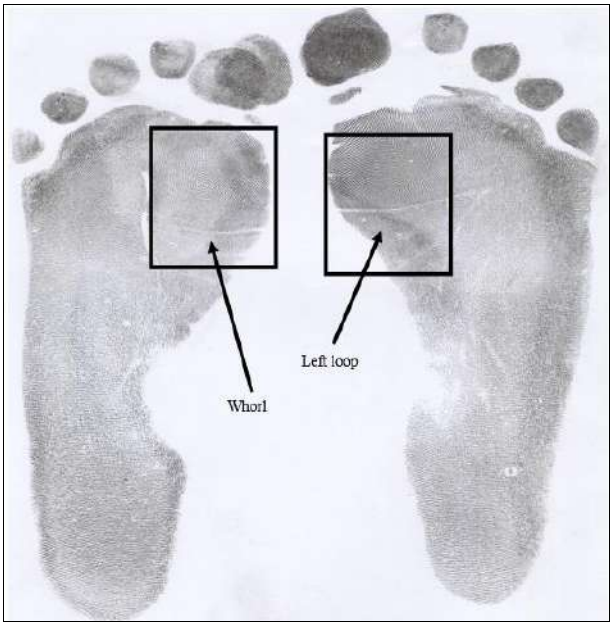

Fig 1: Complete Footprints showing Soleprint regions

3.1 The use of fingerprint recognition algorithm for soleprint

3.1.1. Invert the grayscale of each picture to separate the ridges foreground and backdrop

$$F^{!}_{i,j} = 255 - F_{i,j}\ , i = 1,2, \ldots\ldots M; j = 1,2, \ldots\ldots N \qquad - - - (1)$$

3.1.2. Perform normalization on the images;

$$F^{!!}(X,Y) = \begin{cases} \mu_0 + \dfrac{\sqrt{\sigma_0^2 \,.\, (F^{!}(X,Y) - \mu)^2}}{\sigma^2}\ , if\ F^{!}(X,Y) \geq \mu \\ \mu_0 - \dfrac{\sqrt{\sigma_0^2 \,.\, (F^{!}(X,Y) - \mu)^2}}{\sigma^2}\ , otherwise \ldots\ldots (2) \end{cases}$$

$$Where\ \mu_0 = 100 \Longrightarrow desired\ to\ mean;\ \sigma_0 = 100 \Longrightarrow desired\ variance$$

3.1.3. Apply 2-D Gaussian Smoothing of the form.

$$W(i,j) = \frac{255}{\sum_{i=-(m-1)/2}^{(m-1)/2} \sum_{j=-(m-1)/2}^{(m-1)/2} W(i,j)} \left\{ \frac{1}{2\pi\sigma^2} e^{\frac{1(i^2+j^2)}{2\sigma^2}} \right\},$$

$$-(m-1)/_2 \leq i,j \leq (m-1)/_2 \qquad (3)$$

Obtain 5 X 5 Kernel coefficient from equation (3) for m = 5, σ = 1

$$\therefore W(i,j) = \frac{1}{253} \begin{bmatrix} 1 & 3 & 6 & 3 & 1 \\ 3 & 15 & 25 & 15 & 3 \\ 6 & 25 & 41 & 25 & 6 \\ 3 & 15 & 25 & 15 & 3 \\ 1 & 3 & 6 & 3 & 1 \end{bmatrix}; -2 \leq i,j \leq 2 \qquad (4a)$$

To obtain a Gaussian filtered graphic, multiply equation (4a) by the pictures. In general, the bigger the nucleus, the less apparent the blur. A 5 X 5 matrix, as seen in equation (4a), was used in this work.

Hong, Wan, and Jain (2021) [3] then used the Canny edge detector, an edge detector algorithm employing a multi-stage algorithm to detect various edges in photographs. It was invented in 1986 by John F. Canny. The Gaussian kernel distorts the picture until it is processed by the Canny. The Canny feature senses the main contour boundaries on the files, which are then fed into the device for further processing. The algorithm is made up of five steps;

1. Noise reduction
2. Gradient calculation
3. Non-maximum suppression
4. Double threshold
5. Edge tracking by hysteresis

The Canny mask, as seen in Figure 2, measures the picture in the X and Y directions in 2D space. Two convolution mask operators are used to calculate the gradient.

$$\begin{bmatrix} -1 & -1 \\ 1 & 1 \end{bmatrix} \Longrightarrow GX$$
$$\begin{bmatrix} -1 & 1 \\ -1 & 1 \end{bmatrix} \Longrightarrow GY$$

Fig 2: Illustration of Canny Mask

The gradient procedure returns edge magnitudes or strengths in the X direction GX and the Y direction GY. The equation gives the edge power (4b).

$$|G| = |GX| + |GY| \qquad (4b)$$

3.1.4. Histogram Output the photos are equalized in the following stages.

Using the method, calculate the equalized cumulative frequency;

$$C_K = \left\{ \left[\sum_{j=0}^{K} hist(j) \right] \cdot \left[\frac{L}{MN} \right] \right\} + 0.5 \qquad (5)$$

Remap the intensities of the initial grey picture to the intensities of the equalized image;

$$E^{!!!}(X,Y) = C\left[E^{!!}(X,Y)\right], X = 0,1, \ldots\ldots N; Y = 0,1, \ldots\ldots, M-1 \qquad (6)$$

3.1.5. Separate the Ridge from the Furrow (Valley) such that the minutiae points may be rendered unique by the Binarization method.

Using the form suggested in (Peihao *et al*. 2007), picture binarisation classifies each pixel as a "ridge" (darker) or "valley" (Lighter) (lighter). We add a binarization procedure to an improved picture B (i, j) using the following rules:

1. Assign “ridge’ to pixel (i, j) if B(I, j) ≤ Pk, where *Pk* is the *Kth* percentile of histogram of {B(i, j)}, e.g. *k* = 25 in this case.
2. Assign “valley” to pixel (i, j) if B(i, j). ≥ P_{50},
3. The remaining pixel *{(i,j)}* are classified as “valley” if *B(i,j)* ≥ T_{5x5}, and ‘ridge” otherwise; where T_{5x5} is the

30th percentile of 5x5 pixel values surrounding the pixel (I,J).

3.1.6. Finding the skeleton of the Binarised image via the Thinning procedure is a critical stage in the preprocessing. It makes it easy to find the Minutiae points.

The thinning algorithm mentioned by Zhang and Suen (2019) [8] was used in this case.

The system consists of consecutive passes of two simple measures added to the region's contour points.

A contour point p0 is described as having at least one background pixel in its 8-pixel neighbourhood. If the following criteria apply to a contour point's 8-pixel neighbourhood, it is labelled for deletion in the first pass.

1. The region's neighbour would have a total of 2 to 6 neighbours.
2. Both background-neighbouring neighbours must be connected.
3. p2, p4 or p6 should be in the context
4. p4, p6 or p8 should be in the context

If all criteria are satisfied, the point is designated for deletion. To guarantee that the data structure is not updated during the step's implementation, the point is not discarded before all area points have been processed.

The first two conditions must always hold for a point to be marked for deletion in the second pass of the algorithm, but conditions (c) and (d) are modified as follows.

(C') p2, p4 or p8 should be in the context

(D') p2, p6 or p8 should be in the context

In short, the algorithm adds the following measures iteratively until only the skeleton of the field remains.

1. Phase one involves marking all bottom-right contour points for deletion.
2. Delete all contour points that have been labelled.
3. Stage two involves marking all top-left contour points for deletion.
4. Delete all contour points that have been labelled.

P8	P1	P2
P7	P0	P3
6	P5	P4

(7)

The equation (7) locations are being considered as follows;

P0 = (*x*, *y*). p1= (*x*, *y*-1). P2 = (*x*+1, *y*-1). P3 = (*x*+1, *y*). p4 = (*x*+1, *y*+1). P5 = (*x*, *y*+1). P6 = (*x*-1, *y*+1). P7 = (*x*-1, *y*). p8 = (*x*-1, *y*-1) (8)

Occasionally, ridge boundary aberrations trigger hairy growth (spikes or line fuzz), contributing to spurious or artificial ridge ends and Bifurcation. To restrict this, adaptive morphology filtering is needed (Fitz and Green, 1996) [9] for spike removal after thinning, and this process is referred to as 'pruning' (Jain *et al*., 1995) [10]. 'Dilation' is often a method of filling holes left from previous pre-processing operations. Many post-processing methods focused on basic structural considerations are commonly used to remove many false minutiae that typically impact thinning binary fingerprint pictures.

3.1.7. Image enhancement for poor quality elimination: The efficiency of the minutiae extraction algorithm and other image recognition techniques is highly dependent on the input image quality. Ridges and valleys alternate and flow in a locally steady direction in an ideal picture. Ridges can be easily identified in such cases, and minutiae can be precisely placed in the picture. However, many fingerprint photographs are of poor quality due to skin environments (e.g., damp or dry, cuts and bruises), sensor noise, improper fingerprint friction, and naturally low-quality fingers (e.g., elderly persons, manual workers). There are bound to be images of fine, medium, and low-quality regions within any given broad population of picture (finger, toe, or sole) records (where the ridge pattern is very noisy and corrupted).

An enhancement algorithm aims to increase the visibility of the ridge structures in recoverable regions, thus marking unrecoverable regions as too noisy for further processing and, therefore, should be removed.

For the enhancement of the low-quality images in this work, the approach suggested in (Hong, Wan, and Jain, 2021) [3] based on Gabor filters was selected. Gabor filters have both frequency and orientation selectivity and a joint optimal resolution in both the spatial and frequency domains.

The Gabor filter was built using the even-symmetric actual portion of the original 2D Gabor filter, which was also used in (Hong, 2021) [3] and (Jain, 1991). Consequently,

$$g(x,y,T,\varphi) = exp\left(-\frac{1}{2}\left[\frac{x_\varphi^2}{\sigma_x^2}+\frac{y_\varphi^2}{\sigma_y^2}\right]\right)cos\left(\frac{2\pi x_\varphi}{T}\right) \quad (9)$$

$$x_\varphi = x\cos\varphi + y\sin\varphi \quad (10)$$

$$y_\varphi = -x\sin\varphi + y\cos\varphi \quad (11)$$

Where φ is the derived Gabor filter's direction, and T is the sinusoidal plane wave's period.

The following formula can be deduced by dividing the equation into two orthogonal components, one parallel and one perpendicular to the orientation.

$$g(x,y,T,\varphi) = h_x(x;T,\varphi)\ X\ h_y(y;\varphi)$$

$$= \left\{exp\left(-\frac{x_\varphi^2}{2\sigma_x^2}\right)cos\left(\frac{2\pi x_\varphi}{T}\right)\right\}.\left\{exp\left(-\frac{y_\varphi^2}{2\sigma_y^2}\right)\right\} \quad (12)$$

The first component, *hx*, is a 1-D Gabor function that acts as a band-pass filter, and the second part, *hy*, is a Gaussian function that acts as a low-pass filter.

Finally, a 2D even-symmetric Gabor filter (TGF) conducts low pass filtering along its orientation and band-pass filtering orthogonal to its orientation φ.

3.2 Minutiae Point Detection

Detection of minor flaws the final stage of the binarisation process can be accomplished by using the method suggested by Bansal, Briti, and Punam (2011) [1]: Each ridge pixel in a thinned picture is grouped into one of the following groups based on its 8-connected neighbour. A ridge pixel is referred to as

A. A If a point is isolated since it has no 8 related neighbours, it is said to be isolated.
B. If it has only one 8-connected neighbour, it is an ending.

C. If it has two 8-connected neighbours, it is an edge point.
D. A bifurcation if it has three 8-connected neighbours.
E. A crossing if four 8-connected neighbours surround it.

The crossing number technique was used to remove minutiae. In the equation, the crossing number of pixel 'p' is specified as half the total of the differences between pairs of adjacent pixels representing the 8-neighbourhood of 'p' (13).

$$C_N(p) = \frac{1}{2}\sum_{i=1....8}|val(p_{i\ mod\ 8}) - val(p_{i-1})| \quad (13)$$

Where p0 to p7 are pixels in an ordered series that define p's 8-neighborhood and Val (p) is the pixel value.

4. Results and Discussion

4.1 Implementation Environment

Many methods and algorithms mentioned in this paper were implemented on the Windows 7 operating system using MATLAB R2015b. The tests were carried out on a Pentium(R) 2.20GHz processor with 2.00GB of RAM.

The experiment used one of the 240 soleprint photographs obtained from 120 lepers from nine leper colonies in Nigeria. The TET Fund study grant I recently received allowed me to gather data (2014). Moreover, I am supposed to publish globally as part of the operations.

The fingerprint picture used in the experiment was derived from a previous study I completed as part of my PhD studies at the University of Ilorin in 2010.

Each picture is an 8-bit grey-level image scanned at approximately 600 dpi resolution and 256 256 pixels in size; the image format is a bitmap image compression algorithm. Even though the picture size was not precisely 256 256, the software requires that it be modified to this.

The experiment's aim was not to measure the accuracy of the fingerprint recognition algorithm but rather to analyze the impact of the algorithm on the Soleprint and then equate this effect to a related Fingerprint. This demonstrates that the soleprint may be exposed to the same care as the fingerprint to produce identical results. This is one of the reasons why the execution period was not calculated or taken into account.

The experiment sample collection included Fig. 3(a) Original Soleprint picture -Whorl and Fig. 4(a) Original Fingerprint image -Whorl. The outcomes of the pre-processing and minutiae extraction processes conducted on the Original Soleprint picture (Fig. 3(a)) are depicted in Fig. 3. (b) 3(c) Segmentation, 3(d) Gaussian Blurring, 3(e) Noise Reduction, 3(f) Canny, 3(g) Orientation (h) Binarisation is the process of dividing everything into two parts Fig. 3(i) Thinning, Fig. 3(j) Gabor Filtering, and Fig. 3(k) Minutiae Extraction, For example, see Fig. 4(b) through 4(k), which show identical pre-processing and minutiae extraction effects.

The key pre-processing stage in the fingerprint recognition phase is thinning. A successful thinning process would enable us to obtain more precise minutiae points. The Soleprint and the Fingerprint have a thinning effect, as seen in Figs. 3(i) and 4(i) (image skeleton or 1 pixel thick). Since the two photographs used as a reference series, Fig. 3 and 4 (a), were whorl, the line of direction (local ridge orientation), Fig. 3(g) and Fig. 4(g) were not only identical but often shown to encroach on the image's middle.

Fig 3(a): Original Soleprint Image (Whorl)

Fig 3(b): Segmented Soleprint

Fig 3(c): Normalized Soleprint

Fig 3(d): Gaussian Bluffing of Soleprint

Fig 3(e): Soleprint after Enhancement (Noise Removal)

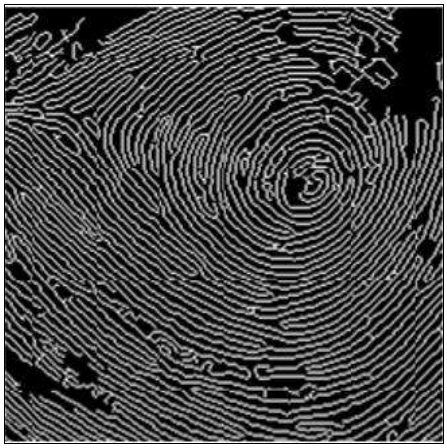

Fig 3(f): Soleprint after Canny

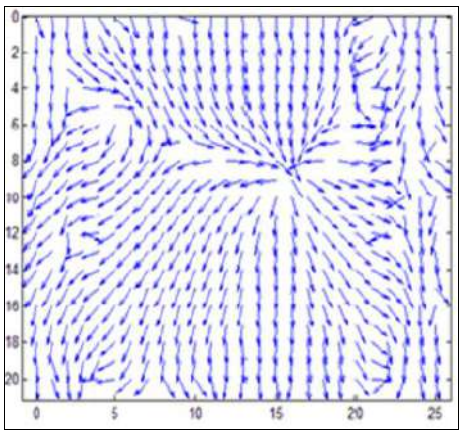

Fig 3(g): Local Ridge Orientation of Soleprint

Fig 3(h): Result of Soleprint Binarization

Fig 3(i): Thinning of the soleprint

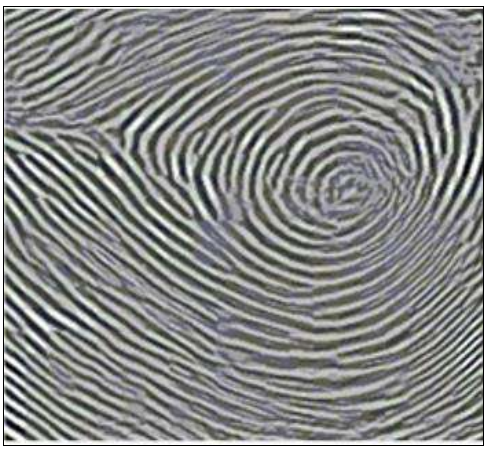

Fig 3(j): Effect of gabor filter on the soleprint

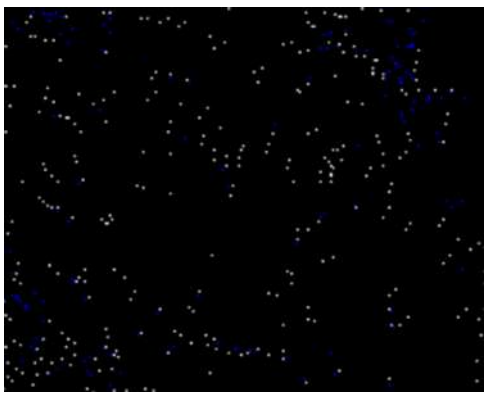

Fig 3(k): Result of Minutiae point detection of Soleprint, Ridge Ending (white), Bifurcation (blue)

Fig 4(a): Original Fingerprint Image (Whorl)

Fig 4 (b): Segmented Fingerprint

Fig 4(c): Normalised Fingerprint

Fig 4(d): Gaussian Blurring of Fingerprint

Fig 4(e): Fingerprint after Enhancement (Noise Removal)

Fig 4(f): Fingerprint after Canny

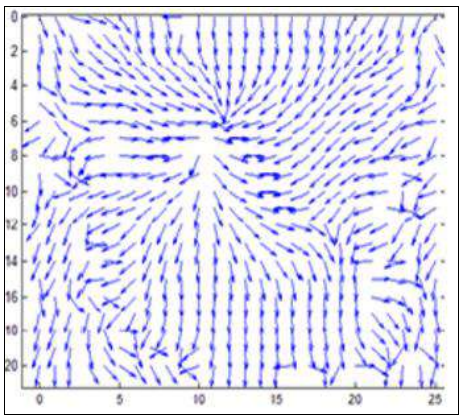

Fig 4(g): Local Ridge Orientation of Fingerprint

Fig 4(h): Result of Fingerprint Binarization

Fig 4(i): Thinning of the fingerprint

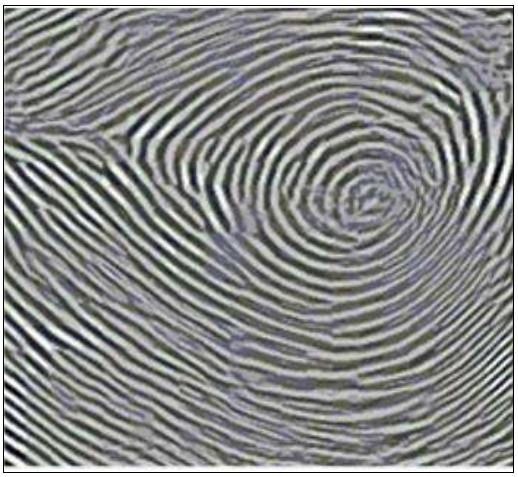

Fig 3(j): Effect of gabor filter on the fingureprint

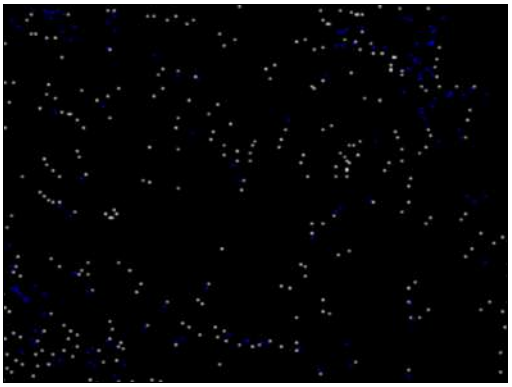

Fig 3(k): Result of Minutiae point detection of fingureprint, Ridge Ending (white), Bifurcation (blue)

5. Conclusion

The experiment showed that, like the fingerprint, the soleprint has the essential characteristics of being peculiar to individuals, including patterns that can yield minutiae marks and, therefore, can be used to distinguish and recognize a person completely. A modern method of personal recognition and voting for lepers and crash patients who do not have a fingerprint is suggested here. The medium is called the Soleprint, a point on the sole adjacent to the big toe, in the flat space right below the toes.

6. Acknowledgements

My heartfelt gratitude goes to the TET Fund, Tertiary Education Trust Fund, in Nigeria, which funded my study on the topic through the National Research Fund scheme.

7. References

1. Bansal Roli, Priti Sehgal, Punam Bedi. Minutiae extraction from fingerprint images-A Review. arXiv preprint arXiv. 2011;1201-1422.
2. Chandan S, Mihir M. DSP Implementation of Fingerprint-Based Biometric System, Part iv Project Final Report, Department of Electrical & Computer Engineering, The University of Auckland; c2020.
3. Hong L, Wan Y, Jain AK. Fingerprint Enhancement Algorithms and Performance Evaluation, IEEE Trans. On pattern, Analysis and Machine Intelligence. 2021;20(8):777-789.
4. Ibiyemi TS, Obaje SE. Automatic Fingerprint and Toeprint Recognition for Personal Identification and Forensic Application". Final Report, Department of Electrical & Electronics Engineering, University of Ilorin; c2010.
5. Jain K, Hong L, Pankanti S, Bolle R. Online Fingerprint Verification, IEEE transaction Pattern Analysis & Machine Intelligence. 2020;19(4):302-313.
6. Maltoni D, Maio D, Jain AK, Prabhakar S. Handbook of Fingerprint Recognition, Springer, New York; c2018.
7. Obaje SE. Lepers Personal Identification Using the Soleprint in Place of Fingerprint. Proceedings of the 3rd International Conference on Electronics and Computer Technology, Kanyakumari, India; c2011, p. V3-471-V3-474.
8. Zhang TY, Suen CY. A Fast Parallel Algorithm for Thinning Digital Pattern, Communications of ACM. 2019;27(3):236-239.
9. Fitz AP, Green RJ. Fingerprint classification using a hexagonal fast Fourier transform. Pattern recognition. 1996 Oct 1;29(10):1587-97.
10. Tiwari S, Singh SM, Jain S. Chronic bilateral suppurative otitis media caused by Aspergillus terreus: Chronische bilaterale suppurative Otitis media durch Aspergillus terreus. Mycoses. 1995 Jul;38(7-8):297-300.